Research Square

Preprints are preliminary reports that have not undergone peer review.
They should not be considered conclusive, used to inform clinical practice,
or referenced by the media as validated information.

Effect of APOE ε4 Genotype on Amyloid-β and Tau Accumulation in Alzheimer's Disease

Min Seok Baek
Department of Neurology, Gangnam Severance Hospital, Yonsei University College of Medicine, Seoul, South Korea
Hanna Cho
Department of Neurology, Gangnam Severance Hospital, Yonsei University College of Medicine, Seoul, South Korea
Hye Sun Lee
Biostatistics Collaboration Unit, Gangnam Severance Hospital, Yonsei University College of Medicine, Seoul, South Korea
Jae Hoon Lee
Department of Nuclear Medicine, Gangnam Severance Hospital, Yonsei University College of Medicine, Seoul, South Korea
Young Hoon Ryu
Department of Nuclear Medicine, Gangnam Severance Hospital, Yonsei University College of Medicine, Seoul, South Korea
Chul Hyoung Lyoo (lyoochel@yuhs.ac)
Department of Neurology, Gangnam Severance Hospital, Yonsei University College of Medicine, Seoul, South Korea
https://orcid.org/0000-0003-2231-672X

Research

Keywords: Alzheimer disease, ApoE, amyloid-β, tau, positron emission tomography

Posted Date: August 12th, 2020

DOI: https://doi.org/10.21203/rs.3.rs-55459/v1

License: This work is licensed under a Creative Commons Attribution 4.0 International License. Read Full License

Version of Record: A version of this preprint was published on October 31st, 2020. See the published version at https://doi.org/10.1186/s13195-020-00710-6.

Abstract

Background

To assess effects of apolipoprotein E (ApoE) ε4 genotype on Aβ and tau burden and their longitudinal changes in Alzheimer's disease (AD) spectrum.

Methods

Among 272 individuals who underwent PET scans (^{18}F-florbetaben for Aβ and ^{18}F-flortaucipir for tau) and ApoE genotyping, 187 individuals completed 2-year follow-up PET scans. After correcting for partial-volume effect, we compared the standardized uptake value ratio (SUVR) for Aβ and tau burden between the ε4 + and ε4- groups. By using a linear mixed-effect model, we measured changes in SUVR in the ApoE ε4 + and ε4- groups.

Results

The ε4 + group showed greater baseline Aβ burden in the diffuse cortical regions and greater tau burden in the lateral, and medial temporal, cingulate, and insula cortices. Tau accumulation rate was higher in the parietal, occipital, lateral, and medial temporal cortices in the ε4 + group. In Aβ + individuals, baseline tau burden was greater in the medial temporal cortex, while Aβ burden was conversely greater in the ε4- group. Tau accumulation rate was higher in the ε4 + group in a small region in the lateral temporal cortex. The effect of ApoE ε4 on enhanced tau accumulation persisted even after adjusting for the global cortical Aβ burden.

Conclusions

Progressive tau accumulation may be more prominent in ε4 carriers, particularly in the medial and lateral temporal cortices. ApoE ε4 allele has differential effects on Aβ burden depending on the existing amyloidosis and enhances vulnerability to progressive tau accumulation in the AD spectrum independent of Aβ.

Background

Except for the rare dominantly inherited Alzheimer's disease (AD), most AD patients are sporadic [1, 2]. The apolipoprotein E (ApoE) gene encodes an 35-kDa extracellular lipid and cholesterol carrier glycoprotein, and its ε4 allele is a major genetic risk factor for sporadic AD [1, 3]. The presence of this allele increases the risk of AD in a dose-dependent manner and lowers the age at onset [4, 5]. However, its effect on the regional accumulation rates of two major pathological proteins—amyloid-β (Aβ) and tau—remains unclear.

Greater amounts of Aβ burden are demonstrated in ε4 carriers than in non-carriers in the previous postmortem and ^{11}C-Pittsburgh compound B (PIB) positron emission tomography (PET) studies [6–8]. Longitudinal change in Aβ burden was also greater in ε4 carriers than non-carriers in the previous studies [9–11], while the other longitudinal study did not find this association [12].

Postmortem studies showed more frequent neurofibrillary tangle pathology in ε4 carriers in a dose-dependent manner [7], a greater tangle pathology in AD patients with ε4 homozygote [13], and an association of ε4 allele with tangle pathology in the presence of Aβ [14]. In contrast, the other study did not find this association [15]. Recent tau PET study exhibited an effect of ApoE ε4 on Aβ-independent increase in tau load in the entorhinal cortex and hippocampus [16],

while the other studies found this effect was associated with the global Aβ burden [17] or even greater tau burden in the prodromal AD and AD dementia patients without ε4 allele, particularly in the parietal cortex, than in ε4 carriers [18].

In this study, we investigated the effects of the ε4 allele on regional Aβ and tau burden and their longitudinal changes in cognitively unimpaired (CU) individuals, mild cognitive impairment (MCI), and AD patients.

Materials And Methods

Participants

From January 2015 to August 2017, 272 individuals completed a baseline tau PET study at Gangnam Severance Hospital. The baseline study included magnetic resonance (MR) and two PET scan (^{18}F-florbetaben for Aβ and ^{18}F-flortaucipir for tau) studies, neuropsychological tests with Seoul Neuropsychological Screening Battery (tests for global cognition and six cognitive domains) [19], and ApoE genotyping. In 187 individuals who agreed to a follow-up study, the same neuroimaging and neuropsychological tests were performed after a mean of 2.0 ± 0.3 years.

We used clinical diagnostic criteria for probable AD dementia proposed by the National Institute of Neurological and Communicative Disorders and Stroke and the Alzheimer's Disease and Related Disorders Association and Petersen's criteria for diagnosing MCI [20, 21]. Thereby, baseline study included 96 CU, 105 MCI and 71 AD dementia patients, and longitudinal study included 80 CU, 42 MCI, and 65 AD dementia patients. Baseline Aβ-positivity was determined by two nuclear medicine specialists using the validated visual assessment methods [22, 23]. Detailed information for the inclusion of participants is described in our previous works [24, 25].

Acquisition of PET and MR images

PET images were acquired in a Biograph mCT PET/CT scanner (Siemens Medical Solutions; Malvern, PA, USA) for 20 min at 90 min after the injection of ^{18}F-florbetaben and at 80 min after the injection of ^{18}F-flortaucipir. Prior to the scan, brain computed tomography images were acquired for attenuation correction. 3D PET images were reconstructed using the ordered-subsets expectation maximization (OSEM) algorithm in a 256 × 256 × 223 matrix with a 1.591 × 1.591 × 1 mm voxel size. In a 3.0 T MR scanner (Discovery MR750, GE Medical Systems, Milwaukee, WI), T1-weighted MR images were acquired using 3D-spoiled gradient-recalled sequences (repetition time = 8.3 ms, echo time = 3.3 ms, flip angle = 12°, 512 × 512 matrix, voxel spacing 0.43 × 0.43 × 1 mm).

Image processing steps

We used FreeSurfer 5.3 (Massachusetts General Hospital, Harvard Medical School; http://surfer.nmr.mgh.harvard.edu) software to obtain participant-specific volumes-of-interest (VOIs). In brief, T1-weighted MR images were resliced to a 1-mm isovoxel space in FreeSurfer, corrected for inhomogeneity and segmented into gray and white matter. After tessellation, 3D-surfaces for gray and white matter were reconstructed. Subcortical regions were segmented with the probabilistic registration method [26], and cortical regions were probabilistically labelled based on the curvature information overlaid on inflated white matter surface [27, 28]. Finally, participant-specific composite VOI images, including 16 and 4 subcortical regions, were created by merging anatomically related regions.

Statistical parametric mapping 12 (Wellcome Trust Centre for Neuroimaging, London, UK) and in-house software implemented in MATLAB 2015b (MathWorks, Natick, MA, USA) were used for the processing of PET images. PET images were first coregistered to MR images resliced to the FreeSurfer isovoxel space. Using participant-specific composite VOI images, PET images were corrected for partial volume effect (PVE) with a region-based voxel-wise (RBV) method [29]. Standardized uptake value ratio (SUVR) images were created using the cerebellar crus median obtained by overlaying a template mask on PET images spatially normalized with diffeomorphic anatomical registration through an

exponentiated lie algebra tool [30]. Finally, regional SUVR values were obtained by overlaying the participant-specific composite VOI images on individual PET images.

For visualization, cortical activities were mapped on the white matter surface by assigning the values of voxels corresponding to the mid-point between the gray and white matter surface, corrected for PVE with the RBV method, and then converted to SUVR maps using the cerebellar crus median as a reference. Surface SUVR images were spatially normalized and finally smoothed on a 2D surface using a Gaussian kernel with 8-mm full-width half-maximum.

Statistical analysis

SPSS 23 (IBM Corp., Armonk, NY, USA) was used for the statistical analysis of demographic data and baseline VOI data. Continuous and categorical demographic variables were compared between the ApoE ε4- and ε4 + groups using independent t-test and chi-square test, respectively. Using the general linear model with age, years of education, sex, and baseline MMSE scores as covariates, baseline SUVR values were compared between the ApoE ε4- and ε4 + groups. *P*-values for trends were calculated using analysis of covariance (ANCOVA) after adjusting for age, sex, years of education, and baseline MMSE scores as covariates. Region-wise multiple comparisons were corrected for using Benjamini-Hochberg's false discovery rate method [31]. Likewise, baseline surface images were compared between the two groups using the same general linear model implemented in FreeSurfer. Longitudinal changes in the regional SUVR values and surface images were compared between the groups using a linear mixed effect model in MATLAB with age, sex, years of education, baseline MMSE scores, and an interaction term between the presence of ApoE ε4 and time intervals as fixed factors under the assumption of a random intercept and slope by setting the intervals and subject as random factors.

Results

Demographic characteristics

Baseline and follow-up demographic data are summarized in Table 1 and e-1. In individuals included in the baseline and follow-up studies, age, sex, and education were not different between the ε4- and ε4 + groups. The ε4 + group showed higher proportions of Aβ-positivity and clinical dementia and worse global cognition measured at baseline than the ε4- group. However, all demographic characteristics and global cognition were not different in each group stratified by Aβ-positivity. Compared to baseline, global cognition worsened at follow-up in both the ε4- and ε4 + groups. The number of ε4 carriers was greater in patients with dementia than that in CU and MCI patients.

Table 1
Baseline demographic characteristics of 272 participants who completed the baseline study

	Aβ±		Aβ-		Aβ+	
	ε4-	ε4+	ε4-	ε4+	ε4-	ε4+
N	195	77	134	24	61	53
Baseline age (years)	70.4 ± 10.3	70.0 ± 8.6	68.4 ± 10.3	65.5 ± 8.3	74.7 ± 8.7	72.1 ± 7.9
Females (%)	127 (65%)	51 (66%)	90 (67%)	16 (67%)	37 (61%)	35 (66%)
Education (years)	11.1 ± 4.9	11.2 ± 5.0	11.0 ± 4.9	11.4 ± 4.2	11.2 ± 4.8	11.1 ± 5.3
Duration (years)	2.6 ± 1.5	3.1 ± 1.4	2.3 ± 1.5	2.4 ± 1.3	3.0 ± 1.5	3.2 ± 1.4
Aβ-positivity (%)	61 (31%)	53 (69%)[a]	0 (0%)	0 (0%)	61 (100%)	53 (100%)
ε2/2 : ε2/3 : ε3/3	1 : 37 : 157	n.a.	1 : 31 : 102	n.a.	0 : 6 : 55	n.a.
ε2/4 : ε3/4 : ε4/4	n.a.	2 : 60 : 15	n.a.	2:21:1	n.a.	0 : 39 : 14
Baseline diagnosis CU/MCI/DEM (%)	79/75/41 (41/38/21%)	17/30/30[a] (22/39/39%)	72/49/13 (54/37/10%)	15/7/2 (63/29/8%)	7/26/28 (11/43/46%)	2/23/28 (4/43/53%)
MMSE	25.4 ± 4.7	23.5 ± 5.3[a]	26.8 ± 3.2	26.7 ± 2.5	22.2 ± 5.7	22.1 ± 5.7
CDR-SB	1.6 ± 2.3	2.7 ± 2.5[a]	0.9 ± 1.5	0.8 ± 1.4	3.1 ± 3.0	3.6 ± 2.4

Data are presented as mean ± SD. [a] $P < 0.05$ for the comparisons between the ε4- and ε4+.

Abbreviations: CU = cognitively unimpaired, MCI = mild cognitive impairment, DEM = dementia, Aβ+/- = Aβ-positivity, ApoE = apolipoprotein-E, MMSE = Mini-Mental State Examination, CDR-SB = Clinical Dementia Rating sum-of-boxes

Baseline Aβ and tau burden

In all 272 individuals, the ApoE ε4 + group exhibited greater Aβ burden in the global cortex, prefrontal, parietal, lateral temporal, parahippocampal, and cingulate cortices and hippocampus than the ε4- group, and all regions survived correcting for multiple comparisons. Conversely, in Aβ + individuals, Aβ burden was greater in the ε4- group in the global cortex, sensorimotor, superior parietal, occipital, and insula cortices than in the ε4 + group, although all regions did not survive correcting for multiple comparisons (Fig. 1A). Surface-based statistics showed similar results as VOI-based comparisons (Fig. 1B).

In all individuals, greater tau burden was observed in the ε4 + group in the lateral and medial temporal, cingulate, and insula cortices, and all regions survived multiple comparisons (Fig. 1A). In Aβ + individuals, the ε4 + group showed greater tau burden in the medial temporal regions, and only the amygdala and hippocampus survived correcting for multiple comparisons. When the baseline global cortical Aβ burden was included as an additional covariate in the model, ApoE ε4 + group exhibited greater tau burden in all medial temporal regions when compared to ε4- group (Additional file 1: Figure S1A). Surface-based statistics showed greater tau burden in the medial temporal and anterior cingulate regions

in the ε4 + group than in the ε4- group, however, none of the regions survived after correcting for multiple comparisons (Fig. 1B).

Increased baseline Aβ burden in the hippocampus was associated with the number of ε4 alleles. Likewise, tau burden in the medial temporal regions showed an association with ε4 allele in a dose-dependent manner (Fig. 4A). In Aβ + individuals, increased tau burden in the hippocampus and amygdala was associated with the ε4 allele in a dose-dependent manner (Fig. 4B).

Longitudinal changes in Aβ and tau burden

Examples of baseline Aβ and tau burden and their changes at follow-up are demonstrated in Fig. 2. In all 187 individuals, the ε4 + group exhibited a higher Aβ accumulation rate than the ε4- group in the global cortex, superior parietal, occipital, lateral temporal, parahippocampal cortices and amygdala, however, none of the regions survived correcting for multiple comparisons (Fig. 3A). A surface-based comparison showed a higher Aβ accumulation rate in the ε4 + group in the diffuse cortical areas than in the ε4- group, and small regions in the lateral temporal cortex survived correcting for multiple comparisons (Fig. 3B). In Aβ + individuals, there was no difference in the Aβ accumulation rate between the two groups.

In all individuals, tau accumulation rate in the ε4 + group was higher in the global cortex, prefrontal, parietal, occipital, lateral and medial temporal, posterior cingulate, and insula cortices compared to the ε4- group. Except for the prefrontal, superior parietal, and posterior cingulate cortices, all regions survived correcting for multiple comparisons (Fig. 3A). In addition, the increase in tau accumulation rate is associated with the number of ApoE ε4 allele (Fig. 4B). Similar to the VOI-based results, a surface-based comparison of the annual increase in tau showed a higher tau accumulation rate, particularly in the diffuse parietotemporal cortex in the ε4 + group (Fig. 3B). In Aβ + individuals, the ε4 + group exhibited a greater annual increase in tau burden in the middle temporal and hippocampus, although none of the regions survived correcting for multiple comparisons (Fig. 3A). Surface-based statistics also showed a higher tau accumulation rate in the small regions in the basal and lateral temporal and sensorimotor cortices (Fig. 3B).

Even after the inclusion of baseline global cortical Aβ burden as an additional covariate in the model, statistical results for the VOI-based comparison of tau accumulation rates between the two ApoE groups were almost similar (Additional file 1: Figure S1B).

Discussion

In this study, we assessed the effects of ApoE ε4 genotype on Aβ and tau burden and found a greater baseline Aβ and tau burden and higher tau accumulation rate in the ε4 + group than in the ε4- group. The Aβ accumulation rate in the ε4 + group was higher in small areas in the lateral temporal cortex. In Aβ + individuals, baseline tau burden in the ε4 + group was greater in the medial temporal regions and tau accumulation rate in the ε4 + group was higher in the small regions in the basal and lateral temporal cortices compared to the ε4- group.

Transgenic mice model with neuron-specific overexpression of ApoE ε4 showed greater phosphorylated tau burden in the neocortex and hippocampus [32], and tau transgenic mice with human ApoE ε4 exhibited greater tau burden in the hippocampus than those with ε2 or ε3 [33]. A postmortem study showed ε4 gene dose-dependent increase in neurofibrillary tangle (NFT) pathology and thereby greater NFT pathology in the diffuse cortical areas in the AD patients with ε4 allele than those without [7]. Another study showed greater cortical NFT pathology only in the AD patients homozygous for ε4 allele than those with a single ε4 allele or those without the allele [13]. Unlike these transgenic mice and human postmortem studies, human cerebrospinal fluid (CSF) biomarker studies showed no differences in the level of CSF T-tau and P-tau between the ε4 + and ε4- groups [34, 35]. Moreover, one cross-sectional tau PET study in Aβ + MCI

and AD patients demonstrated that the ε4- group conversely exhibited greater tau burden in the parieto-occipital cortex than the ε4 + group [18]. However, our study results showed greater tau burden in the medial temporal areas even in the Aβ + individuals with the ε4 allele than in those without, although the result for the hippocampus was limited by the off-target binding in the choroid plexus neighboring hippocampus. This discrepancy may be attributable to the disproportionate frequency of the ε4 allele in different subtypes of AD. The hippocampal sparing type of AD is associated with a younger age at onset, lower frequency of the ApoE ε4 allele, greater tau burden particularly in the parietal cortex, faster cortical atrophy, and faster cognitive decline than the typical AD subtype [36–39]. Therefore, we suspect that the inclusion of a greater proportion of the hippocampal sparing subtype in the study cohort diluted an effect of ε4 on tau burden or even caused contrary results.

Although there has been a report demonstrating a longitudinal increase in CSF tau in AD patients [40], one longitudinal tau PET study in a small number of AD patients did not find an association between the ApoE genotypes and longitudinal changes in tau burden [41]. In our results for all Aβ ± individuals, the regional tau accumulation rate was higher in the ε4 + group in the diffuse regions in the medial and lateral temporal and parieto-occipital cortices than that in the ε4- group. Moreover, even in the Aβ + individuals, higher tau accumulation rate was observed in the ε4 + group in the small regions in the temporal cortex suggesting the impact of ApoE ε4 genotype on progressive tau accumulation.

One recent tau PET study including 325 individuals (90% cognitively-unimpaired and 10% cognitively-impaired) showed an association of ApoE ε4 with increased tau burden in the entorhinal cortex, but they lost significance after adjusting for global cortical Aβ burden [17]. In contrast, the other study including 489 individuals with more balanced distribution of cognitive status (57% cognitively-unimpaired and 43% cognitively-impaired) demonstrated an effect of ApoE ε4 on increased tau burden in the entorhinal cortex and hippocampus, and it persisted even after adjusting for global cortical Aβ burden like our study result [16]. Moreover, the effect of ApoE ε4 on progressive tau accumulation was replicated after adjusting for global cortical Aβ burden in our longitudinal study. Therefore, tau accumulation may be accelerated by the presence of ApoE ε4 independent of Aβ burden.

The ApoE ε4 isoform was more likely to stimulate neuronal Aβ production than the other isoforms *in vitro* [42], and transgenic mice expressing the ApoE ε4 isoform showed less effective clearance of soluble Aβ from the brain interstitial fluid [43]. Human autopsy findings demonstrated greater Aβ burden in the ε4 + than in the ε4- group not only in AD patients [13], but also in the MCI patients and CU individuals [44]. Likewise, when compared to the individuals without the ε4 allele, a greater Aβ burden was observed in the global cortex in CU and MCI patients with ε4 allele [8], and in the temporo-parietal cortex in AD patients with ε4 allele in the PET studies [45]. Our study also demonstrated greater Aβ burden in the diffuse cortical areas in individuals with the ε4 allele than in those without. In contrast to the strong association between the ε4 allele and baseline Aβ burden, we found a weak effect of ApoE ε4 on progressive Aβ accumulation in small regions in the lateral temporal cortex only in all Aβ ± individuals. The Aβ accumulation rate in the Aβ + individuals was not different between the ε4 + and ε4- groups like previous studies [9, 11], suggesting an effect of the ApoE ε4 allele on Aβ deposition only in the early stage of the disease.

Interestingly, Aβ burden in the Aβ + individuals was paradoxically greater in the ε4- group than in the ε4 + group, similar to the previous ^{11}C-PIB and ^{18}F-fluorodeoxyglucose PET studies that demonstrated lower Aβ burden and contrarily greater cortical hypometabolism in the AD patients with ε4 allele than in those without [46, 47]. This paradoxical effect of the ApoE ε4 allele on Aβ deposition can be expected by clinical studies that found an impact of the ApoE ε4 allele on Aβ burden in CU and MCI but not in those with AD [8, 34]. Furthermore, a study with transgenic mice demonstrated enhanced Aβ aggregation by ApoE4 in the early seeding stage but not in the later Aβ growth stage [48]. An *in vitro* experiment demonstrated that ApoE ε4 binds to toxic Aβ oligomers and more potently delays further aggregation of Aβ into the PET-detectable fibril form than the other ApoE isoforms [49]. Therefore, ApoE ε4 may play an important role in Aβ accumulation in the early stages of AD pathogenesis rather than in the advanced stages and may be more likely to be

exposed to toxic oligomers. Subsequently, events toward final neurodegeneration may be induced, thereby shifting the hypothetical biomarker curves for tau and neurodegeneration to the Aβ curve [47]. It is also interesting to note that a transgenic mice model expressing both Aβ and tau exhibited a smaller number of plaque than that expressing only Aβ [50]. Greater microgliosis and reduction of the amyloid-precursor protein-producing neurons due to greater tau accumulation in ε4 carriers may be another possible mechanism explaining the paradoxically lower Aβ burden [50]. However, this hypothesis cannot fully explain the mechanism due to mismatch between the cortical areas with greater Aβ burden in the ε4- group and those with greater tau burden in the ε4 + group (Fig. 1).

Limitations

This study has several limitations. First, different time intervals for each participant between baseline and follow-up studies (mean of 2.0 ± 0.3 years) may affect the results, however, the linear mixed effect model with random intercept and slope adopted in this study was considered more appropriate for the study design with variable time intervals compared to the repeated measures-ANOVA test. In addition, longer follow up duration would be promising to observe more conclusive pathologic changes between the ε4 + and ε4- groups.

Conclusions

Our study revealed that progressive tau accumulation occurs more prominently in ε4 carriers, particularly in the medial and lateral temporal cortices. The presence of the ε4 allele not only has differential effects on Aβ burden depending on the existing amyloidosis but also enhances vulnerability to progressive tau accumulation in the AD spectrum independent of Aβ.

Abbreviations

ApoE
apolipoprotein E;
CU
cognitively unimpaired;
MCI
mild cognitive impairment;
SUVR
Standardized uptake value ratio;

Declarations

Ethics approval and consent to participate

This study was approved by the institutional review board of Gangnam Severance Hospital (Ref# 3-2017-0054), and written informed consent was obtained from all participants and/or their legal guardians. All procedures performed in this study were in accordance with the ethical standards of the 1964 Helsinki declaration and its later amendments.

Consent for publication

Not applicable

Availability of data and materials

Data generated by this study are available from the corresponding author on reasonable request. The data are not publicly available due to privacy restriction.

Competing interests

The authors declare that they have no competing interests

Funding

This research was supported by a faculty research grant of Yonsei University College of Medicine for (6-2018-0068), a grant from the 2020 Research Grant of Gangnam Severance Hospital Research Committee, Basic Science Research Program through the National Research Foundation of Korea (NRF) funded by the Ministry of Education (NRF2020R1F1A1076154 & NRF2018R1D1A1B07049386), and a grant of the Korea Health Technology R&D Project through the Korea Health Industry Development Institute (KHIDI) funded by the Ministry of Health & Welfare, Republic of Korea (Grant number : HI18C1159).

Authors' contributions

MSB contributed with: conception and design, collection and assembly of data, data analysis and interpretation, and manuscript writing. HC contributed with: collection and assembly of data, and data analysis and interpretation. HSL contributed with: data analysis and interpretation. JHL contributed with: collection and assembly of data, data analysis and interpretation. YHR contributed with: conception and design, administrative support, collection and assembly of data, data analysis and interpretation, manuscript writing, and final approval of manuscript. CHL contributed with: conception and design, administrative support, and final approval of manuscript.

Acknowledgements

We express our special appreciation to Tae Ho Song and Won Taek Lee (PET technologists) who managed all PET scans with enthusiasm.

References

1. Scheltens NME, Tijms BM, Koene T, Barkhof F, Teunissen CE, Wolfsgruber S, et al. Cognitive subtypes of probable Alzheimer's disease robustly identified in four cohorts. Alzheimers Dement. 2017;13(11):1226–36.
2. Crane PK, Trittschuh E, Mukherjee S, Saykin AJ, Sanders RE, Larson EB, et al. Incidence of cognitively defined late-onset Alzheimer's dementia subgroups from a prospective cohort study. Alzheimers Dement. 2017;13(12):1307–16.
3. Munoz SS, Garner B, Ooi L. Understanding the Role of ApoE Fragments in Alzheimer's Disease. Neurochem Res. 2019;44(6):1297–305.
4. Liu CC, Liu CC, Kanekiyo T, Xu H, Bu G. Apolipoprotein E and Alzheimer disease: risk, mechanisms and therapy. Nat Rev Neurol. 2013;9(2):106–18.
5. Corder EH, Saunders AM, Strittmatter WJ, Schmechel DE, Gaskell PC, Small GW, et al. Gene dose of apolipoprotein E type 4 allele and the risk of Alzheimer's disease in late onset families. Science. 1993;261(5123):921–3.
6. Rebeck GW, Reiter JS, Strickland DK, Hyman BT. Apolipoprotein E in sporadic Alzheimer's disease: allelic variation and receptor interactions. Neuron. 1993;11(4):575–80.

7. Sabbagh MN, Malek-Ahmadi M, Dugger BN, Lee K, Sue LI, Serrano G, et al. The influence of Apolipoprotein E genotype on regional pathology in Alzheimer's disease. BMC Neurol. 2013;13(1):44.
8. Rowe CC, Ellis KA, Rimajova M, Bourgeat P, Pike KE, Jones G, et al. Amyloid imaging results from the Australian Imaging, Biomarkers and Lifestyle (AIBL) study of aging. Neurobiol Aging. 2010;31(8):1275–83.
9. Villemagne VL, Pike KE, Chetelat G, Ellis KA, Mulligan RS, Bourgeat P, et al. Longitudinal assessment of Abeta and cognition in aging and Alzheimer disease. Ann Neurol. 2011;69(1):181–92.
10. Mishra S, Blazey TM, Holtzman DM, Cruchaga C, Su Y, Morris JC, et al. Longitudinal brain imaging in preclinical Alzheimer disease: impact of APOE epsilon4 genotype. Brain. 2018;141(6):1828–39.
11. Lim YY, Mormino EC. Alzheimer's Disease Neuroimaging I. APOE genotype and early beta-amyloid accumulation in older adults without dementia. Neurology. 2017;89(10):1028–34.
12. Resnick SM, Bilgel M, Moghekar A, An Y, Cai Q, Wang MC, et al. Changes in Abeta biomarkers and associations with APOE genotype in 2 longitudinal cohorts. Neurobiol Aging. 2015;36(8):2333–9.
13. Tiraboschi P, Hansen LA, Masliah E, Alford M, Thal LJ, Corey-Bloom J. Impact of APOE genotype on neuropathologic and neurochemical markers of Alzheimer disease. Neurology. 2004;62(11):1977–83.
14. Farfel JM, Yu L, De Jager PL, Schneider JA, Bennett DA. Association of APOE with tau-tangle pathology with and without beta-amyloid. Neurobiol Aging. 2016;37:19–25.
15. Landen M, Thorsell A, Wallin A, Blennow K. The apolipoprotein E allele epsilon 4 does not correlate with the number of senile plaques or neurofibrillary tangles in patients with Alzheimer's disease. J Neurol Neurosurg Psychiatry. 1996;61(4):352–6.
16. Therriault J, Benedet AL, Pascoal TA, Mathotaarachchi S, Chamoun M, Savard M, et al. Association of Apolipoprotein E epsilon4 With Medial Temporal Tau Independent of Amyloid-beta. JAMA Neurol. 2020;77(4):470–9.
17. Ramanan VK, Castillo AM, Knopman DS, Graff-Radford J, Lowe VJ, Petersen RC, et al. Association of Apolipoprotein E varepsilon4, Educational Level, and Sex With Tau Deposition and Tau-Mediated Metabolic Dysfunction in Older Adults. JAMA Netw Open. 2019;2(10):e1913909.
18. Mattsson N, Ossenkoppele R, Smith R, Strandberg O, Ohlsson T, Jogi J, et al. Greater tau load and reduced cortical thickness in APOE epsilon4-negative Alzheimer's disease: a cohort study. Alzheimers Res Ther. 2018;10(1):77.
19. Kang Y, Na DL. Seoul Neuropsychological Screening Battery (SNSB). Incheon. South Korea: Human Brain Research & Consulting Co.; 2003.
20. McKhann G, Drachman D, Folstein M, Katzman R, Price D, Stadlan EM. Clinical diagnosis of Alzheimer's disease: report of the NINCDS-ADRDA Work Group under the auspices of Department of Health and Human Services Task Force on Alzheimer's Disease. Neurology. 1984;34(7):939–44.
21. Petersen RC, Smith GE, Waring SC, Ivnik RJ, Tangalos EG, Kokmen E. Mild cognitive impairment: clinical characterization and outcome. Arch Neurol. 1999;56(3):303–8.
22. Sabri O, Sabbagh MN, Seibyl J, Barthel H, Akatsu H, Ouchi Y, et al. Florbetaben PET imaging to detect amyloid beta plaques in Alzheimer's disease: phase 3 study. Alzheimers Dement. 2015;11(8):964–74.
23. Villemagne VL, Ong K, Mulligan RS, Holl G, Pejoska S, Jones G, et al. Amyloid imaging with (18)F-florbetaben in Alzheimer disease and other dementias. J Nucl Med. 2011;52(8):1210–7.
24. Cho H, Choi JY, Hwang MS, Kim YJ, Lee HM, Lee HS, et al. In vivo cortical spreading pattern of tau and amyloid in the Alzheimer disease spectrum. Ann Neurol. 2016;80(2):247–58.
25. Cho H, Choi JY, Hwang MS, Lee JH, Kim YJ, Lee HM, et al. Tau PET in Alzheimer disease and mild cognitive impairment. Neurology. 2016;87(4):375–83.
26. Fischl B, Salat DH, Busa E, Albert M, Dieterich M, Haselgrove C, et al. Whole brain segmentation: automated labeling of neuroanatomical structures in the human brain. Neuron. 2002;33(3):341–55.

27. Desikan RS, Segonne F, Fischl B, Quinn BT, Dickerson BC, Blacker D, et al. An automated labeling system for subdividing the human cerebral cortex on MRI scans into gyral based regions of interest. Neuroimage. 2006;31(3):968–80.
28. Fischl B, van der Kouwe A, Destrieux C, Halgren E, Segonne F, Salat DH, et al. Automatically parcellating the human cerebral cortex. Cereb Cortex. 2004;14(1):11–22.
29. Thomas BA, Erlandsson K, Modat M, Thurfjell L, Vandenberghe R, Ourselin S, et al. The importance of appropriate partial volume correction for PET quantification in Alzheimer's disease. Eur J Nucl Med Mol Imaging. 2011;38(6):1104–19.
30. Ashburner J. A fast diffeomorphic image registration algorithm. Neuroimage. 2007;38(1):95–113.
31. Benjamini Y, Hochberg Y. Controlling the False Discovery Rate - a Practical and Powerful Approach to Multiple Testing. Journal of the Royal Statistical Society Series B-Statistical Methodology. 1995;57(1):289–300.
32. Brecht WJ, Harris FM, Chang S, Tesseur I, Yu GQ, Xu Q, et al. Neuron-specific apolipoprotein e4 proteolysis is associated with increased tau phosphorylation in brains of transgenic mice. J Neurosci. 2004;24(10):2527–34.
33. Shi Y, Yamada K, Liddelow SA, Smith ST, Zhao L, Luo W, et al. ApoE4 markedly exacerbates tau-mediated neurodegeneration in a mouse model of tauopathy. Nature. 2017;549(7673):523–7.
34. Morris JC, Roe CM, Xiong C, Fagan AM, Goate AM, Holtzman DM, et al. APOE predicts amyloid-beta but not tau Alzheimer pathology in cognitively normal aging. Ann Neurol. 2010;67(1):122–31.
35. Lautner R, Palmqvist S, Mattsson N, Andreasson U, Wallin A, Palsson E, et al. Apolipoprotein E genotype and the diagnostic accuracy of cerebrospinal fluid biomarkers for Alzheimer disease. JAMA Psychiatry. 2014;71(10):1183–91.
36. Murray ME, Graff-Radford NR, Ross OA, Petersen RC, Duara R, Dickson DW. Neuropathologically defined subtypes of Alzheimer's disease with distinct clinical characteristics: a retrospective study. Lancet Neurol. 2011;10(9):785–96.
37. Ossenkoppele R, Lyoo CH, Sudre CH, van Westen D, Cho H, Ryu YH, et al. Distinct tau PET patterns in atrophy-defined subtypes of Alzheimer's disease. Alzheimers Dement. 2020;16(2):335–44.
38. Sluimer JD, Vrenken H, Blankenstein MA, Fox NC, Scheltens P, Barkhof F, et al. Whole-brain atrophy rate in Alzheimer disease: identifying fast progressors. Neurology. 2008;70(19 Pt 2):1836–41.
39. Risacher SL, Anderson WH, Charil A, Castelluccio PF, Shcherbinin S, Saykin AJ, et al. Alzheimer disease brain atrophy subtypes are associated with cognition and rate of decline. Neurology. 2017;89(21):2176–86.
40. Blomberg M, Jensen M, Basun H, Lannfelt L, Wahlund LO. Increasing cerebrospinal fluid tau levels in a subgroup of Alzheimer patients with apolipoprotein E allele epsilon 4 during 14 months follow-up. Neurosci Lett. 1996;214(2–3):163–6.
41. Harrison TM, La Joie R, Maass A, Baker SL, Swinnerton K, Fenton L, et al. Longitudinal tau accumulation and atrophy in aging and alzheimer disease. Ann Neurol. 2019;85(2):229–40.
42. Huang YA, Zhou B, Wernig M, Sudhof TC. ApoE2, ApoE3, and ApoE4 Differentially Stimulate APP Transcription and Abeta Secretion. Cell. 2017;168(3):427–41. e21.
43. Castellano JM, Kim J, Stewart FR, Jiang H, DeMattos RB, Patterson BW, et al. Human apoE isoforms differentially regulate brain amyloid-beta peptide clearance. Sci Transl Med. 2011;3(89):89ra57.
44. Caselli RJ, Walker D, Sue L, Sabbagh M, Beach T. Amyloid load in nondemented brains correlates with APOE e4. Neurosci Lett. 2010;473(3):168–71.
45. Drzezga A, Grimmer T, Henriksen G, Muhlau M, Perneczky R, Miederer I, et al. Effect of APOE genotype on amyloid plaque load and gray matter volume in Alzheimer disease. Neurology. 2009;72(17):1487–94.
46. Ossenkoppele R, van der Flier WM, Zwan MD, Adriaanse SF, Boellaard R, Windhorst AD, et al. Differential effect of APOE genotype on amyloid load and glucose metabolism in AD dementia. Neurology. 2013;80(4):359–65.

47. Lehmann M, Ghosh PM, Madison C, Karydas A, Coppola G, O'Neil JP, et al. Greater medial temporal hypometabolism and lower cortical amyloid burden in ApoE4-positive AD patients. J Neurol Neurosurg Psychiatry. 2014;85(3):266–73.
48. Liu CC, Zhao N, Fu Y, Wang N, Linares C, Tsai CW, et al. ApoE4 Accelerates Early Seeding of Amyloid Pathology. Neuron. 2017;96(5):1024–32 e3.
49. Garai K, Verghese PB, Baban B, Holtzman DM, Frieden C. The binding of apolipoprotein E to oligomers and fibrils of amyloid-beta alters the kinetics of amyloid aggregation. Biochemistry. 2014;53(40):6323–31.
50. DeVos SL, Corjuc BT, Commins C, Dujardin S, Bannon RN, Corjuc D, et al. Tau reduction in the presence of amyloid-beta prevents tau pathology and neuronal death in vivo. Brain. 2018;141(7):2194–212.

Figures

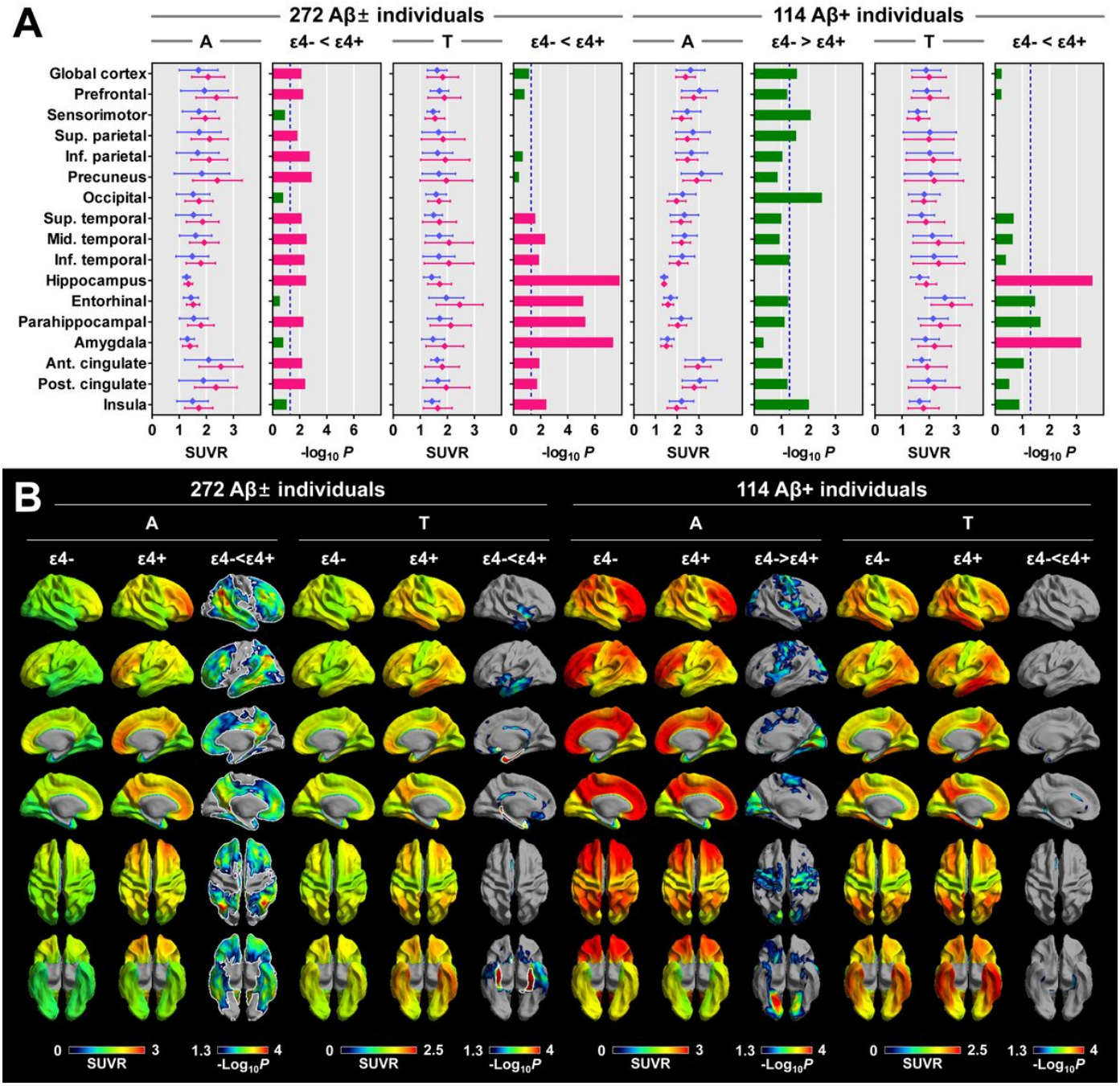

Figure 1

Comparison of baseline 18F-florbetaben and 18F-flortaucipir SUVR between the ApoE ε4- and ε4+ groups. (A) VOI-based comparisons between the ApoE ε4- and ε4+ groups. Data are presented as means (dots) and standard deviations (error bars) of the ε4- (blue) and ε4+ (red) groups. P-values for the comparison between the ε4- and ε4+ groups are expressed as -Log10P. Red bars represent the regions that survived correcting for region-wise multiple comparisons (false discovery rate-corrected P < 0.05), and blue dotted lines represent uncorrected P = 0.05. (B) Surface-based comparisons between the ApoE ε4- and ε4+ groups. Regions surrounded by white lines (ε4-<ε4+ in Aβ and tau burden in all individuals) represent the cortical areas that survived correcting for multiple comparisons (false discovery rate-corrected P < 0.05). P-values for the comparison between the ε4- and ε4+ groups are expressed as -Log10P. Abbreviations: Aβ+/- = Aβ-positivity, ApoE = apolipoprotein-E, SUVR = standardized uptake value ratio, A = 18F-florbetaben, T = 18F-flortaucipir

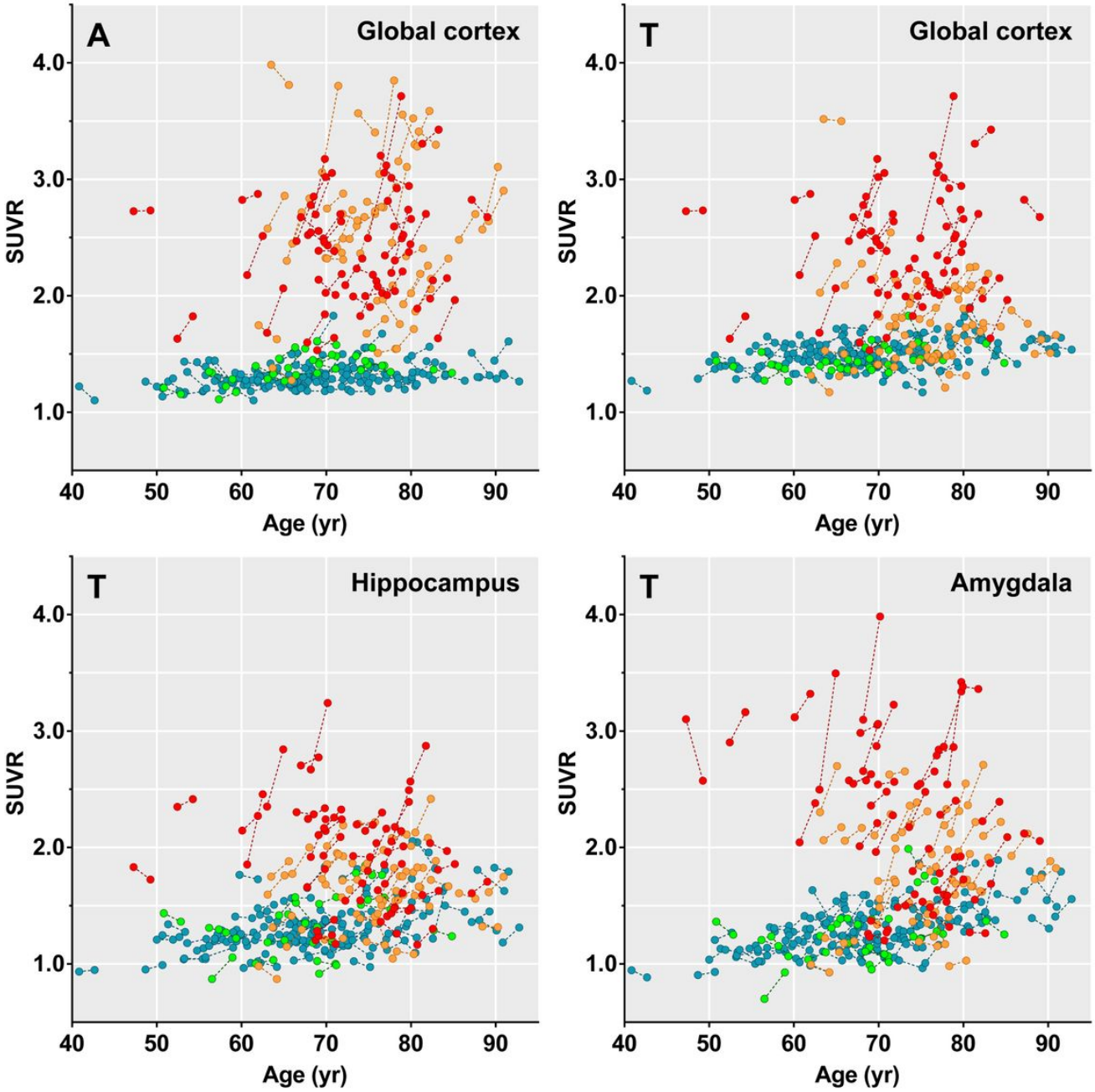

Figure 2

Spaghetti plots showing individual changes in regional SUVR values In 187 Aβ± individuals, the individual data points measured at baseline and follow-up are displayed as color-coded dots (cyan = Aβ- / ApoE ε4-, green = Aβ- / ApoE ε4+, orange = Aβ+ / ApoE ε4-, red = Aβ+ / ApoE ε4+). Abbreviations: Aβ+/- = Aβ-positivity, ApoE = apolipoprotein-E, SUVR = standardized uptake value ratio, A = 18F-florbetaben, T = 18F-flortaucipir

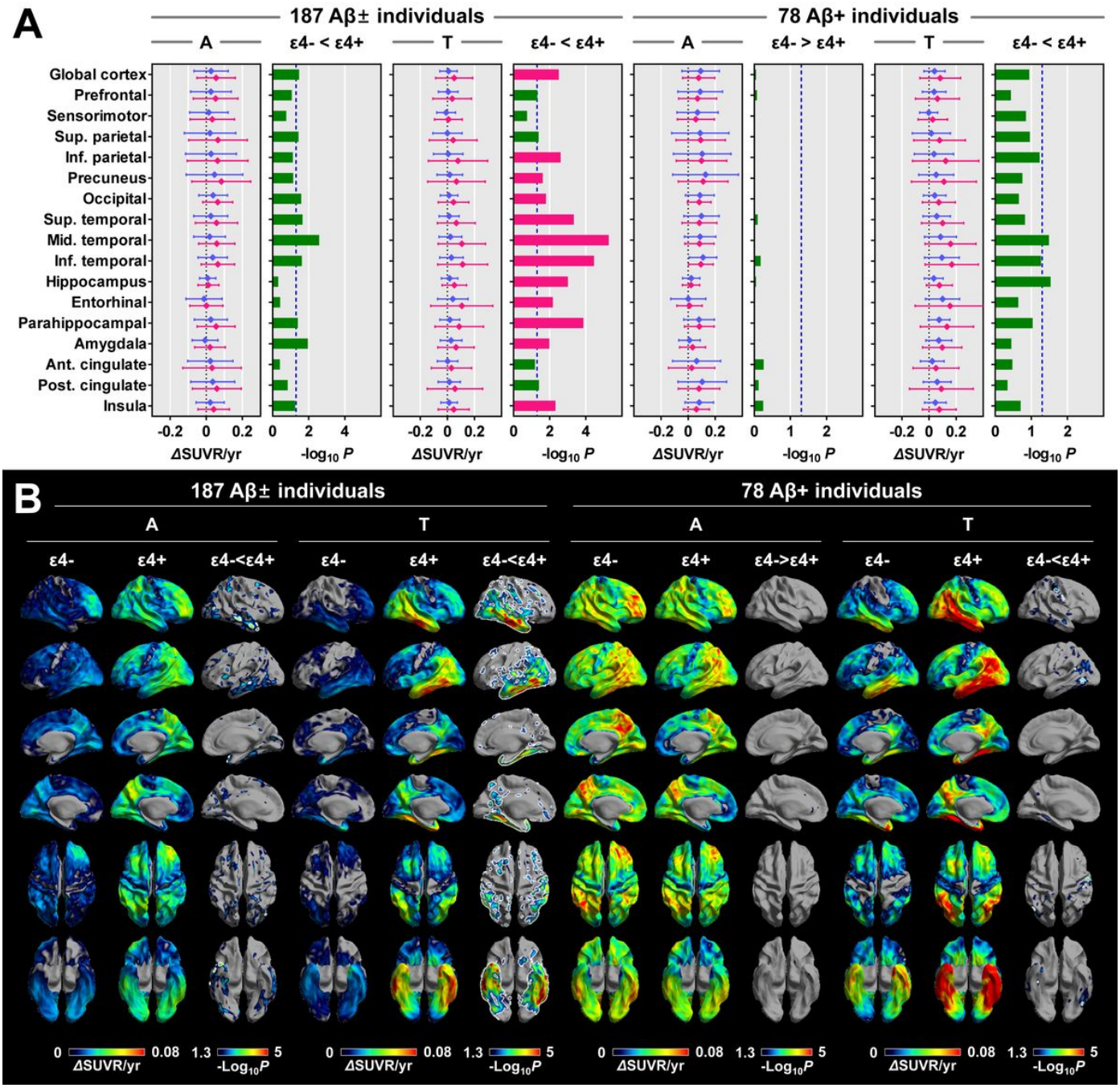

Figure 3

Comparison of annual changes in 18F-florbetaben and 18F-flortaucipir SUVR between the ApoE ε4- and ε4+ groups. (A) VOI-based comparison between the ApoE ε4- and ε4+ groups. Data are presented as means (dots) and standard deviations (error bars) of the ε4- (blue) and ε4+ (red) groups. P-values for the comparison between the ε4- and ε4+ groups are expressed as -Log10P. Red bars represent the regions that survived correcting for region-wise multiple comparisons (false discovery rate-corrected P < 0.05), and blue dotted lines represent uncorrected P = 0.05. (B) Surface-based comparisons between the ApoE ε4- and ε4+ groups. Regions surrounded by white lines (ε4-<ε4+ in Aβ and tau accumulation rates in all individuals, and ε4-<ε4+ in tau accumulation rate in Aβ+ individuals) represent the cortical

areas that survived correcting for multiple comparisons (false discovery rate-corrected P < 0.05). P-values for the comparison between the ε4- and ε4+ groups are expressed as -Log10P. P-values for the comparison between the baseline and follow-up are expressed as -Log10P. Abbreviations: Aβ+/- = Aβ-positivity, ApoE = apolipoprotein-E, SUVR = standardized uptake value ratio, A = 18F-florbetaben, T = 18F-flortaucipir

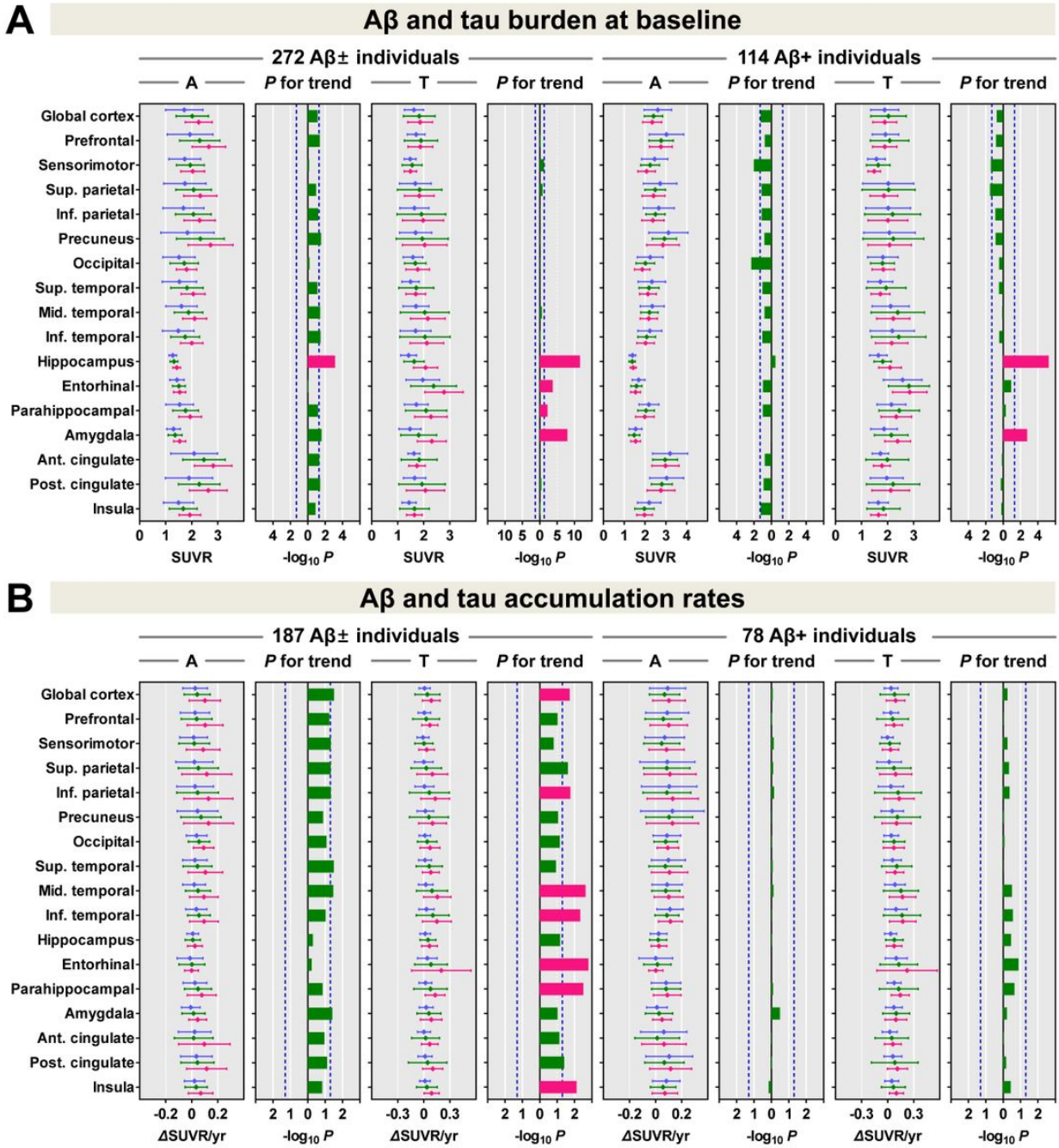

Figure 4

P for trend analysis of baseline 18F-florbetaben and 18F-flortaucipir SUVR and their longitudinal accumulation rates across the ApoE ε4-negative, heterozygous, and homozygous groups. Data are presented as means and standard deviations (error bars) of ε4-negative (blue), ε4-heterozygous (green), and ε4-homogygous (red) groups. Regions that showed significant differences in a dose-dependent manner after adjusting for sex, age, duration of education, and MMSE score (uncorrected P for trend < 0.05) and additionally survived correcting for region-wise multiple comparisons (false discovery rate-corrected P < 0.05) are presented as red bars. Blue dotted lines represent uncorrected P for trend = 0.05. Rightward direction of horizontal bars represents an SUVR values increased with higher numbers of ε4 alleles,

while the leftward direction represents a SUVR values decreased with higher numbers of ε4 alleles. Abbreviations: Aβ+/- = Aβ-positivity, ApoE = apolipoprotein-E, SUVR = standardized uptake value ratio, A = 18F-florbetaben, T 18F-flortaucipir.

Supplementary Files

This is a list of supplementary files associated with this preprint. Click to download.

- Additionalfile1.doc